ChemPubSoc Europe

DOI: 10.1002/chem.201904580

CHEMISTRY A European Journal Full Paper

Metallotweezers | *Hot Paper* |

# Discrete Supramolecular Stacks Based on Multinuclear Tweezer-Type Rhodium Complexes

Bei-Bei Guo,[a] Mohammad Azam,[b] Saud I. AlResayes,[b] Yue-Jian Lin,[a] and Guo-Xin Jin*[a]

*Dedicated to Professor Kazuyuki Tatsumi on the occasion of his 70th birthday*

**Abstract:** By taking advantage of self-complementary π–π stacking and CH–π interactions, a series of discrete quadruple stacks were constructed through the self-aggregation of U-shaped dirhodium metallotweezer complexes featuring various planar polyaromatic ligands. By altering the conjugate stacking strength and bridging ligands, assemblies with a range of topologies were obtained, including a binuclear D-shaped macrocycle, tetranuclear open-ended cagelike frameworks, and duplex metallotweezer stacking structures. Furthermore, a rare stacking interaction resulting in selective C–H activation was observed during the self-assembly process of these elaborate architectures.

## Introduction

Noncovalent intra- and intermolecular interactions occur frequently in programmed biological and chemical processes,[1–4] such as protein folding, (bio)catalysis, and molecular recognition, and are a major research focus in the field of artificial supramolecular chemistry. These interactions are always weak but specific, and play significant roles in product assembly by controlling the ordered combination of building blocks. Based on this principle, numerous examples of this type of precise control over product assembly have been reported over the past few decades,[5–7] such as the construction of molecular knots, links, shuttles, and stacked aromatics, and this has greatly extended the available libraries of programmed topological structures. In addition, important processes such as recognition, chemical transport, and catalysis have also been expressed in these structures. Therefore, the ability to utilize and modulate noncovalent interactions in a rational manner has been a significant goal in the design of supramolecular architectures.

In an effort to mimic complex biological processes, the synthesis of molecular machines with specific functionalities has attracted wide attention. Therein, molecular tweezers play a key role due to their interesting recognition properties, in which their open cavities allow guest binding through a variety of noncovalent interactions, such as π–π stacking, hydrogen bonding, and electrostatic effects. The term "molecular tweezers" was introduced in 1978 by Whitlock and Chen, and such species are characterized by two identical flat arms in a *syn* conformation linked by a significantly rigid tether.[4] The average separation between two arms of about 7 Å facilitates complexation with aromatic substrates through π–π interactions and endows the tweezers with diverse properties.

In addition to specific noncovalent interactions, metal–ligand coordination has also played a leading role in the programmed design of metallasupramolecules. These dynamic bonds provide the possibility of predefining a product assembly due to the often predictable coordination geometries of the applied metal units. However, whereas the majority of the reported tweezers feature purely organic structures,[8,9] metallotweezer structures are limited.[10,11] Nevertheless, metal-based tweezers have gradually attracted attention throughout the last two decades, mainly due to their mild and concise synthesis relative to traditional organic receptors.

Half-sandwich [Cp*M] (M = Ir, Rh)[12,13] units have proven to be excellent building blocks for the construction of supramolecules. Although a variety of topological structures based on these units have been assembled by following well-established design principles, the preparation of molecular tweezers based on [Cp*M] fragments remains a gap in this research field. Furthermore, although we and others have demonstrated that products formed by C–H activation are usually unique assemblies and structurally stable due to the robust M–C bonds formed,[14] the self-assembly of metallasupramolecules involving C–H activation has in general been ignored, has thus far resulted in structures with relatively conventional topologies, and hence is in need of expansion.

Herein, by taking advantage of controllable, selective C–H activation of conjugate proligands, a series of discrete quadru-

[a] B-B. Guo, Dr. Y.-J. Lin, Prof. Dr. G.-X. Jin
Shanghai Key Laboratory of Molecular Catalysis and Innovative Materials
State Key Laboratory of Molecular Engineering of Polymers
Department of Chemistry, Fudan University, Shanghai 200433 (P.R. China)
E-mail: gxjin@fudan.edu.cn

[b] Dr. M. Azam, S. I. AlResayes
Department of Chemistry, College of Science
King Saud University, PO BOX 2455, Riyadh 11451 (KSA)

Supporting information and the ORCID identification number(s) for the author(s) of this article can be found under: https://doi.org/10.1002/chem.201904580.


© 2020 Wiley-VCH Verlag GmbH & Co. KGaA, Weinheim

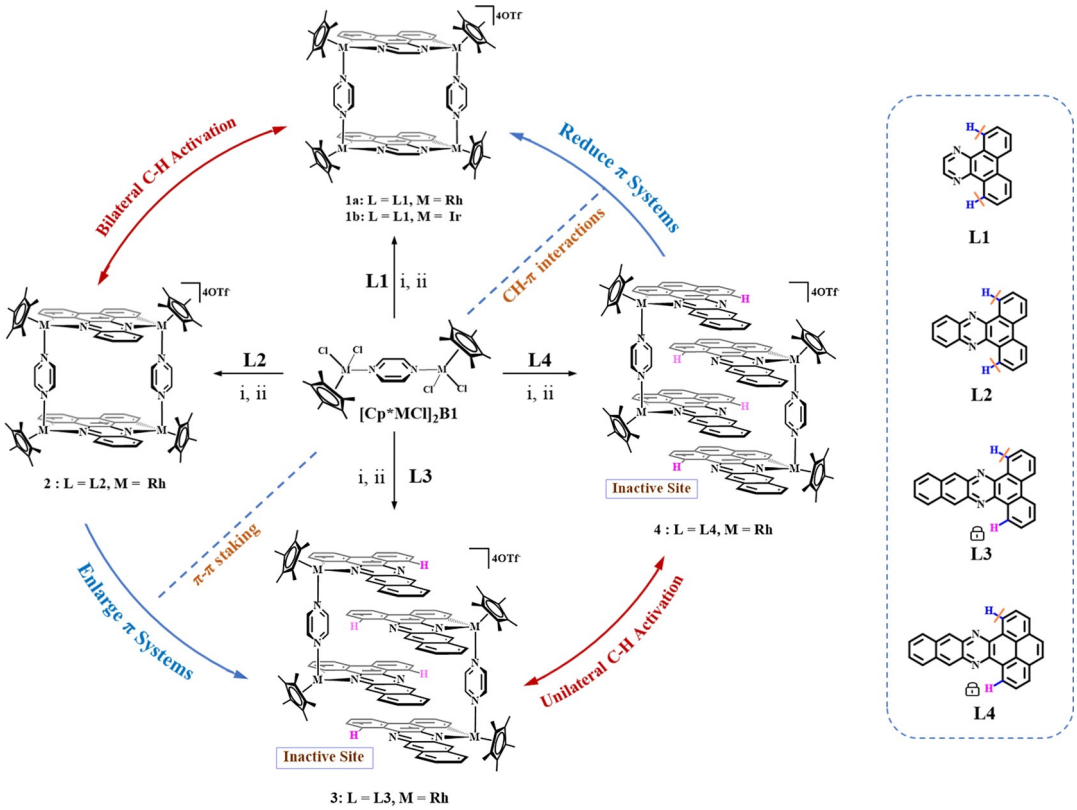


**Scheme 1.** Synthesis of tetranuclear rectangles **1** and **2** and duplex metallotweezer stacks **3** and **4**. Novel stacking interactions resulting from selective unilateral C–H activations of **L3** and **L4** were observed due to the formation of duplex metallotweezer stacks structures in **3** and **4**. i) AgOTf, 12 h; ii) **L**, NaOAc, 12 h.

ple stacks featuring RhCp* units were constructed by noncovalent self-aggregation of rare U-shaped dirhodium metallotweezer complexes. Four similar conjugated polycyclic proligands (**L1**, **L2**, **L3**, **L4**) with gradually enlarged π systems (Scheme 1) were investigated and compared in subsequent C–H-activation-directed self-assembly, in which they had distinct effects on the final supramolecular architectures. Firstly, the rigid building block $[Cp^*MCl]_2$**B1** (M = Rh, Ir) (Scheme 1), with a metal–metal separation of about. 7 Å was selected.[15] With the different polycyclic proligands employed, tetranuclear rectangle or duplex metallotweezer structures were assembled, in which the proligands underwent bilateral (**L1**, **L2**) or unilateral (**L3**, **L4**) C–H activation. The assembly process was also attempted with longer and more flexible bridging ligand **B2** (Scheme 2), unlocking the bilateral C–H activation of proligand **L3**, and thus D-shaped binuclear macrocycles were formed.

As a result of selective C–H activation, D-shaped macrocycles, open-ended cagelike rectangles, and unprecedented quadruple stacks based on metallotweezers were obtained simply by selection of bidentate bridging ligands with different lengths and flexibilities or polyaromatic proligands with different sizes of π systems in the assembly process.

## Results and Discussion

Four similar, conjugated, heterocyclic proligands (**L1**–**L4**) with different sizes of π systems were selected (Scheme 1). Bridges **B1** and **B2**, of different length and flexibility, were employed in subsequent assemblies (Scheme 2). NMR spectra, ESI-MS, and elemental analysis were used to characterize the obtained compounds.

The binuclear $[Cp^*MCl_2]_2$**B1** (M = Rh, Ir) building block was obtained by the reaction of $[\{Cp^*MCl_2\}_2]$ with pyrazine at room temperature, followed by treatment with $Ag(CF_3SO_3)$ for 12 h. Subsequently, the smallest conjugated polyaromatic ligand, **L1**, was added to the mixture with sodium acetate under a nitrogen atmosphere. The color change of the solution from yellow to dark red indicated progress of the base-promoted C–H activation reaction. After stirring for 12 h, the solution was filtered and concentrated, and red products **1a** and **1b** were obtained in 85 and 87% yield, respectively, after extraction with diethyl ether. Single crystals of complex **1a** were obtained by slow liquid-phase diffusion of *n*-hexane into its saturated dichloromethane solution at ambient temperature, and single crystals of **1b** were obtained by vapor diffusion of diethyl ether into its concentrated acetonitrile solution. Structural analysis of crystals of **1a** and **1b** revealed the formation of tetranuclear open-ended cagelike frameworks (Figure 1 and Figure S1 in the Supporting Information), in which two pyrazine bridging ligands support two roughly parallel **L1** planes with bilateral C–H bonds undergoing activation. The cagelike frameworks of **1a** and **1b** encapsulate one molecule of dichloromethane or acetonitrile, respectively, in their cavities during the crystallization processes. However, as determined by NMR spectroscopy, the


© 2020 Wiley-VCH Verlag GmbH & Co. KGaA, Weinheim

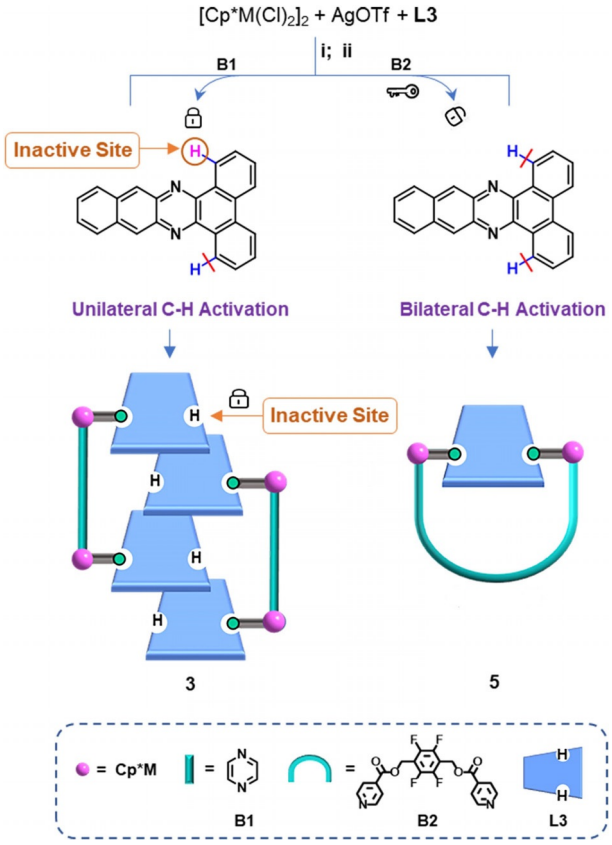


**Scheme 2.** Skeleton representation of tweezer dimer **3** and macrocycle **5**. Utilization of longer and more flexible bridging ligand **B2** instead of **B1** unlocked the bilateral C–H activation of proligand **L3** in the assembly process to form binuclear macrocycle **5**. i) NaOAc, 12 h; ii) **B**, 12 h.

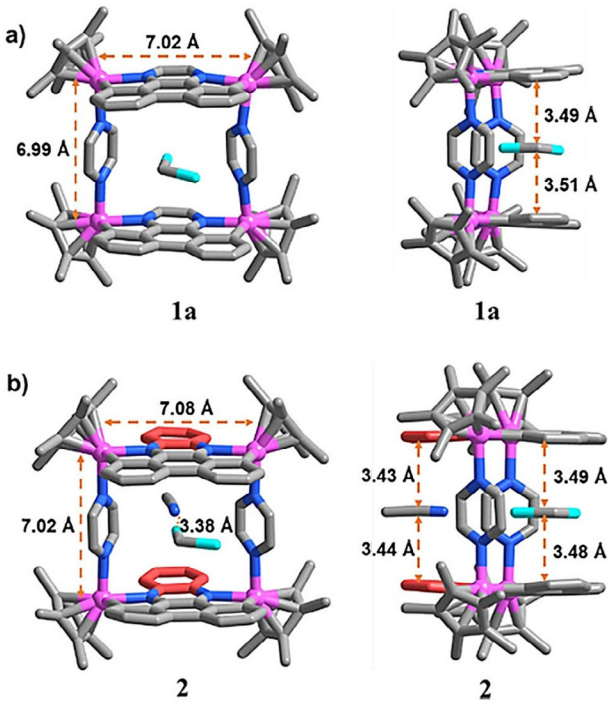


**Figure 1.** Crystallographically derived structures of a) **1a** and b) **2**. All hydrogen atoms and counterions are omitted for clarity. Color code: N blue, C gray, Rh violet, Cl cyan; red: additional π systems of proligand **L2**.

guest molecules captured in the crystalline state are released from the host frameworks on dissolution due to weak host–guest interactions in solution.

An additional fused benzene ring was introduced to form polyaromatic ligand **L2** with larger π system. A synthetic procedure similar to that used to prepare complex **1a** was carried out for the assembly of complex **2** with **L2** instead of **L1**. Thereby, **2** was obtained as a red solid in 83% yield, and was also determined to have an open-ended cagelike structure (Figure 1). Compared with **1**, the capacity for encapsulation of the resulting framework has been improved due to the extended ligand **L2**, and two different solvent molecules (one acetonitrile and one dichloromethane) are encapsulated concurrently during the crystallization process. Similarly, the guest molecules of **2** are also released on dissolution.

To explore the potential of such proligands with large conjugated systems in subsequent assemblies, ligand **L2** was further extended in the synthesis of ligand **L3**, with a length of 10.82 Å, which we predicted might enable stronger noncovalent interactions. By following the synthetic procedures and reactant molar ratios applied above and employing **L3** instead of **L1**/**L2**, red product **3** was obtained in an uncharacteristically low yield. Moreover, its NMR spectra are much more complex than those of the aforementioned macrocycles **1** and **2**. The $^1$H NMR spectra of **3** exhibited two similar sets of signals in $CDCl_3$, which were attributed to a single diffusion coefficient ($D = 3.6 \times 10^{-10}$ m$^2$ s$^{-1}$) by means of $^1$H DOSY NMR spectroscopy.

Single crystals of **3** were obtained by diffusion of diethyl ether into a concentrated solution in acetonitrile/dichloromethane and analyzed by XRD. Unexpectedly, in the solid-state structure of **3**, discrete quadruple stacks were formed by the intercalation of two U-shaped dirhodium metallotweezers (Figure 2). Each tweezer component is composed of two identical, parallel arms derived from proligand **L3** in a *syn* conformation and one rigid bridging pyrazine ligand with a distance

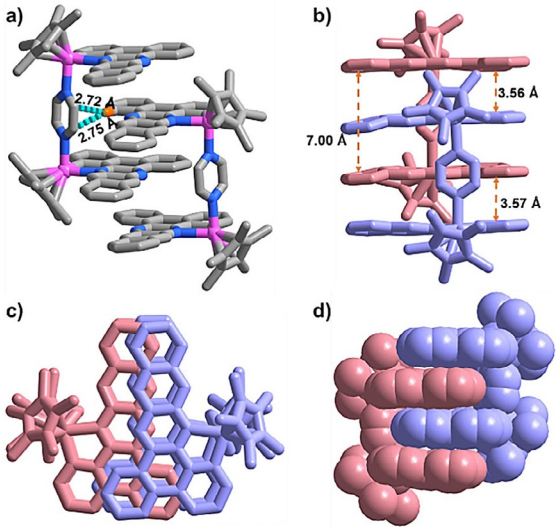


**Figure 2.** a) Crystal structure of **3**. b) Side view. c) Top view. d) Space-filling mode. All counterions and other hydrogen atoms are omitted for clarity. Color code: N blue, C gray, Rh violet, H orange.


© 2020 Wiley-VCH Verlag GmbH & Co. KGaA, Weinheim

of about 7 Å between metal centers. This separation provides the perfect distance for each metallotweezer to engage the other by way of π–π stacking interactions. The edge-to-face CH–π interactions between certain hydrogen atoms of the inner **L3** units and the bridging ligands **B1** further stabilize this quadruple stack.

In contrast to the bilateral C–H activation of proligands **L1**/**L2** in assemblies **1** and **2**, the larger polyaromatic proligand **L3** undergoes only single C–H activation in the construction of **3**. Blocking of the C–H site through the noncovalent interactions in the quadruple stack **3** is assumed to protect the second activation site from further activation, despite the presence of excess reactant and ample reaction time. Furthermore, modification of the reactant molar ratios (ratio of $[Cp^*RhCl]_2$**B1** to **L3** = 1:2) led to improved yields of **3** (79%).

The unusual behavior of **L3** in the assembly of **3** was further investigated. In place of short and rigid bridge **B1**, the long and flexible bridge **B2** was introduced in a subsequent assembly. The $[\{Cp^*IrCl_2\}_2]$**B2** building block was prepared by the reaction of $[\{Cp^*IrCl_2\}_2]$ with bridge **B2** and further employed in the construction of the binuclear D-shaped macrocycle **5** (Scheme 3). The skeletal structure of **5** is provided in Figure S2 in the Supporting Information, derived from imperfect crystal data recorded by XRD. A similar construct could be also obtained when Rh centers were used instead of Ir centers.

Whereas one reaction site of **L3** remained inactive to further activation in **3**, ligand **L3** plays a more conventional bilateral C–H activation role in the assembly of **5**. This contrast further highlights the shielding of a potential C–H activation site of **L3** by noncovalent interactions observed in the formation of discrete quadruple stack **3**, and also demonstrates a rare stacking interaction directed by selective C–H activation to assemble supramolecular stacks based on duplex metallotweezer structures.

To confirm the effect of noncovalent interactions on these assembly processes, this study was further extended by replacement of ligand **L3** with the longer polyaromatic ligand **L4**. A similar synthetic procedure to that used to prepare **3** was followed in the synthesis of **4**, but by using **L4** in the place of **L3**. In the $^1$H DOSY NMR spectrum of **4**, a single diffusion coefficient ($D = 5.5 \times 10^{-10}$ m$^2$ s$^{-1}$) corresponding to the two distinct sets of signals was observed in $CD_3CN$. As expected, discrete quadruple-stack structure **4** was constructed by noncovalent stacking of two dirhodium metallotweezer complexes, the solid-state structure of which was determined by XRD (Figure 3).

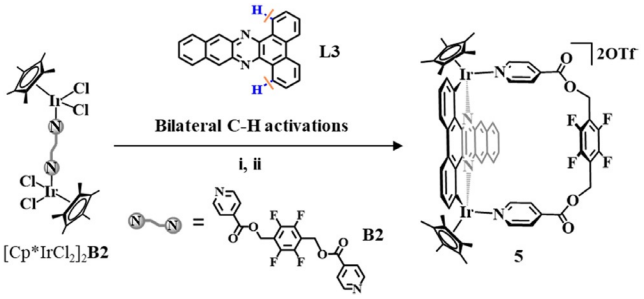


**Scheme 3.** Synthesis of binuclear macrocycle **5** by bilateral C–H activation of proligand **L3**. i) NaOAc, 12 h; ii) **B**, 12 h.

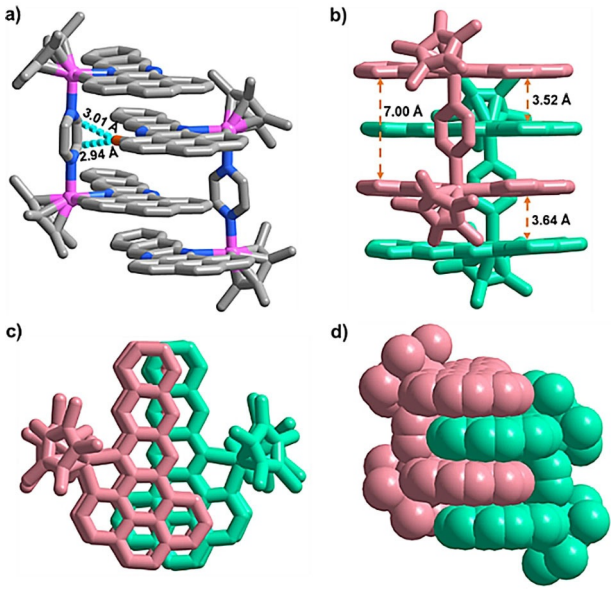


**Figure 3.** a) Crystal structure of **4**. b) Side view. c) Top view. d) Space-filling mode. All counterions and other hydrogen atoms are omitted for clarity. Color code: N blue, C gray, Rh violet, H orange.

## Conclusion

Through simple alteration of planar polyaromatic proligands **L1**–**L4** with gradually enlarged π systems, a series of discrete supramolecular architectures with different topologies has been rationally constructed due to the different strengths of stacking interactions, including a binuclear D-shaped macrocycle, tetranuclear open-ended cagelike frameworks, and rare duplex metallotweezer stacked structures. The construction of the duplex assemblies can be attributed to noncovalent intermolecular interactions inducing self-complementarity. Moreover, selective C–H activation has been observed in these assemblies. In the case of proligands **L1**/**L2** with smaller fused conjugate systems, tetranuclear frameworks were obtained through bilateral self-assembly directed by C–H activation. In contrast, by employing the larger conjugated proligands **L3**/**L4**, exclusive formation of duplex metallotweezer structures through unilateral activation of each ligand was observed, thanks to noncovalent interactions favoring the discrete quadruple-stack structures. Overall, this contribution has demonstrated a self-assembly approach to stacking interactions directed by selective C–H activation and thus provides a foundation for the design and construction of molecular tweezers and discrete aromatic stacks.

## Experimental Section

### General considerations

All manipulations were performed under a nitrogen atmosphere by using standard Schlenk techniques. Solvents were freshly dis-


© 2020 Wiley-VCH Verlag GmbH & Co. KGaA, Weinheim

tilled by standard procedures prior to use. Once the reactions were finished, the obtained compounds were air-stable and were subsequently handled without precautions. [{Cp*IrCl$_2$}$_2$] (M = Rh, Ir, Cp* = $\eta^5$-pentamethylcyclopentadienyl),[16] proligands **L1**–**L4**,[17,18] and bridging ligand **B2**[19] (Scheme 3) were prepared according to previously reported literature methods. Other reagents were purchased from commercial sources and used without further purification. $^1$H, $^1$H-$^1$H COSY, and $^1$H DOSY NMR spectra were measured with a Bruker AVANCE III HD spectrometer at room temperature. ESI mass spectra were recorded with a Micro TOF II mass spectrometer. Elemental analysis was performed with an Elementar Vario EL III analyzer after drying samples at 328 K under vacuum for 24 h.

### Preparation of 1 a

Bridging ligand **B1** (8.0 mg, 0.1 mmol) was added to a solution of [{Cp*RhCl$_2$}$_2$] (62.2 mg, 0.1 mmol) in $CH_2Cl_2$ (20 mL) at room temperature. After vigorous stirring for 6 h, Ag($CF_3SO_3$) (102.8 mg, 0.4 mmol) was added. The mixture was stirred in the dark at room temperature overnight, and then **L1** (23.0 mg, 0.1 mmol) and NaOAc (41.0 mg, 0.5 mmol) were added to the solution, and the mixture was again stirred for 12 h. The solution was then filtered and concentrated in a rotary evaporator. After extraction with diethyl ether, the red product was separated by centrifugation and dried under vacuum (85% yield). $^1$H NMR (400 MHz, $CD_3CN$, ppm): 9.16 (s, 4H, **L1**-H), 8.17 (s, 8H, pyrazine-H), 8.13 (d, $J$ = 4.0 Hz, 4H, **L1**-H), 8.10 (d, $J$ = 8.0 Hz, 4H, **L1**-H), 7.74 (t, $J$ = 8.0 Hz, 4H, **L1**-H), 1.62 (s, 60H, Cp*-H); ESI-MS: $m/z$ = 2015.1595 (calcd for $[C_{84}H_{84}F_{12}Rh_4N_8O_{12}S_4-OTf]^+$: 2015.1594); elemental analysis (%) calcd for elemental analysis (%) calcd for $C_{84}H_{84}F_{12}Rh_4N_8O_{12}S_4$ ($M$ = 2165.48): C 46.59, H 3.91, N 5.17; found: C 46.54, H 3.87, N 5.20.

### Preparation of 1 b

The synthesis of **1 b** was carried out similarly to that of **1 a**, with the use of [{Cp*IrCl$_2$}$_2$] (80.0 mg, 0.1 mmol) instead of [{Cp*RhCl$_2$}$_2$], which was obtained as a red solid in 87% yield. $^1$H NMR (400 MHz, $CDCl_3$, ppm): 9.24 (s, 4H, **L1**-H), 8.46 (s, 8H, pyrazine-H), 8.20 (d, $J$ = 4.0 Hz, 4H, **L1**-H), 8.08 (d, $J$ = 8.0 Hz, 4H, **L1**-H), 7.77 (t, $J$ = 8.0 Hz, 4H, **L1**-H), 1.71 (s, 60H, Cp*-H); ESI-MS: $m/z$ = 2373.3883 (calcd for $[C_{84}H_{84}F_{12}Ir_4N_8O_{12}S_4-OTf]^+$: 2373.3873); elemental analysis (%) calcd for $C_{84}H_{84}F_{12}Ir_4N_8O_{12}S_4$ ($M$ = 2522.72): C 39.99, H 3.36, N 4.44; found: C 39.95, H 3.41, N 4.49.

### Preparation of 2

The synthesis of **2** was carried out similarly to that of **1 a**, with the use of **L2** (28.0 mg, 0.1 mmol) instead of **L1** (23.1 mg, 0.1 mmol), and **2** was obtained as a red solid in 83% yield. $^1$H NMR (400 MHz, $CD_3CN$, ppm): 8.68 (m, 4H, **L2**-H), 8.41 (m, 4H, **L2**-H), 8.22 (d, $J$ = 8.0 Hz, 4H, **L2**-H), 8.08 (d, $J$ = 8.0 Hz, 4H, **L2**-H), 7.82 (s, 8H, pyrazine-H), 7.73 (t, $J$ = 8.0 Hz, 4H, **L2**-H), 1.61 (s, 60H, Cp*-H); elemental analysis (%) calcd for $C_{92}H_{88}F_{12}Rh_4N_8O_{12}S_4$ ($M$ = 2265.59): C 48.77, H 3.92, N 4.95; found: C 48.80, H 3.87, N 4.91.

### Preparation of 3

Pyrazine (8.0 mg, 0.1 mmol) was added to a solution of [{Cp*RhCl$_2$}$_2$] (62.2 mg, 0.1 mmol) in $CH_2Cl_2$ (20 mL) at room temperature. After vigorous stirring for 6 h, Ag($CF_3SO_3$) (102.8 mg, 0.4 mmol) was added. The mixture was stirred in the dark at room temperature overnight, and then **L3** (66.0 mg, 0.2 mmol) and NaOAc (82.0 mg, 1.0 mmol) were added to the solution and the mixture was again stirred for 12 h. The solution was then filtered and concentrated with a rotary evaporator. The red product **3** was separated by centrifugation and dried under vacuum, after extraction with diethyl ether, in 79% yield. $^1$H NMR (400 MHz, $CDCl_3$, ppm): 9.27 (d, $J$ = 4.0 Hz, 4H, pyrazine-H), 9.13 (s, 2H, **L3**-H), 9.04 (d, $J$ = 4.0 Hz, 4H, pyrazine-H), 8.88 (s, 2H, **L3**-H), 8.62 (d, $J$ = 12.0 Hz, 2H, **L3**-H), 8.44 (d, $J$ = 4.0 Hz, 2H, **L3**-H), 8.37 (d, $J$ = 8.0 Hz, 2H, **L3**-H), 8.31 (d, $J$ = 12.0 Hz, 2H, **L3**-H), 7.71 (t, $J$ = 8.0 Hz, 2H, **L3**-H), 7.59–7.55 (m, 4H, **L3**-H), 7.48 (d, $J$ = 8.0 Hz, 2H, **L3**-H), 7.43 (t, $J$ = 8.0 Hz, 2H, **L3**-H), 7.32 (t, $J$ = 8.0 Hz, 2H, **L3**-H), 7.25 (d, $J$ = 8.0 Hz, 2H, **L3**-H), 7.09 (t, $J$ = 8.0 Hz, 2H, **L3**-H), 6.93 (d, $J$ = 8.0 Hz, 2H, **L3**-H), 6.81 (t, $J$ = 8.0 Hz, 2H, **L3**-H), 6.78 (s, 2H, **L3**-H), 6.71 (d, $J$ = 8.0 Hz, 2H, **L3**-H), 6.55 (d, $J$ = 8.0 Hz, 2H, **L3**-H), 6.47 (t, $J$ = 8.0 Hz, 2H, **L3**-H), 6.31 (t, $J$ = 8.0 Hz, 2H, **L3**-H), 6.29 (d, $J$ = 8.0 Hz, 2H, **L3**-H), 6.22 (d, $J$ = 8.0 Hz, 2H, **L3**-H), 5.37 (s, 2H, **L3**-H), 4.13 (t, $J$ = 8.0 Hz, 2H, **L3**-H), 3.33 (d, $J$ = 8.0 Hz, 2H, **L3**-H), 1.99 (s, 30H, Cp*-H), 1.57 (s, 30H, Cp*-H); $^1$H NMR (400 MHz, [D$_6$]DMSO, ppm): 9.31 (s, 2H, pyrazine-H), 9.28 (d, $J$ = 8.0 Hz, 2H, **L3**-H), 8.84 (s, 2H, pyrazine-H), 8.77 (d, $J$ = 8.0 Hz, 2H, **L3**-H), 8.66 (s, 2H, **L3**-H), 8.55 (d, $J$ = 8.0 Hz, 2H, **L3**-H), 8.52 (d, $J$ = 8.0 Hz, 2H, **L3**-H), 8.48 (d, $J$ = 8.0 Hz, 2H, **L3**-H), 8.15 (d, $J$ = 8.0 Hz, 2H, **L3**-H), 7.97 (d, $J$ = 8.0 Hz, 2H, **L3**-H), 7.91–7.82 (m, 10H, **L3**-H), 1.63 (s, 30H, Cp*-H); elemental analysis (%) calcd for $C_{148}H_{120}F_{12}Rh_4N_{12}O_{12}S_4$ ($M$ = 3026.47): C 58.73, H 4.00, N 5.55; found: C 58.77, H 3.98, N 5.49.

### Preparation of 5

The synthesis of **5** was carried out similarly to that of **1 b**, with the use of **B2** (42.0 mg, 0.1 mmol) instead of **B1** (8.0 mg, 0.1 mmol), and **L3** (33.0 mg, 0.1 mmol) instead of **L1** (23.0 mg, 0.1 mmol). Compound **5** was obtained as a red solid in 74% yield. $^1$H NMR (400 MHz, $CDCl_3$, ppm): 9.57 (s, $J$ = 8.0 Hz, 2H, **L3**-H), 8.69 (d, $J$ = 4.0 Hz, 2H, **L3**-H), 8.41 (d, $J$ = 8.0 Hz, 2H, **L3**-H), 8.25 (d, $J$ = 4.0 Hz, 4H, pyridyl-H), 8.16 (d, $J$ = 8.0 Hz, 2H, **L3**-H), 8.06 (d, $J$ = 8.0 Hz, 2H, **L3**-H), 7.86 (t, $J$ = 8.0 Hz, 2H, **L3**-H), 7.47 (d, $J$ = 4.0 Hz, 4H, pyridyl-H), 4.46 (d, $J$ = 8.0 Hz, 2H, **B2**), 4.21 (d, $J$ = 8.0 Hz, 2H, **B2**), 1.97 (s, 30H, Cp*-H); ESI-MS: $m/z$ = 1553.2847 (calcd for $[C_{66}H_{54}F_{10}Ir_2N_4O_{10}S_2-OTf]^+$: 1553.2856), 702.1659 (calcd for $[C_{66}H_{54}F_{10}Ir_2N_4O_{10}S_2-2OTf]^{2+}$: 702.1666); Elemental analysis (%) calcd for $C_{66}H_{54}F_{10}Ir_2N_4O_{10}S_2$ ($M$ = 1701.70): C 46.58, H 3.20, N 3.29; found: C 46.62, H 3.17, N 3.35.

### Preparation of 4

The synthesis of **4** was carried out similarly to that of **3**, with the use of **L4** (70.8 mg, 0.2 mmol) instead of **L3** (66.0 mg, 0.2 mmol). Compound **4** was obtained as a red solid in 82% yield. $^1$H NMR (400 MHz, $CD_3CN$, ppm): 9.00 (d, $J$ = 4.0 Hz, 4H, pyrazine-H), 8.91 (s, 2H, **L4**-H), 8.82 (s, 2H, **L4**-H), 8.78 (d, $J$ = 4.0 Hz, 4H, pyrazine-H), 8.51–8.47 (m, 5H, **L4**-H), 8.41 (d, $J$ = 8.0 Hz, 2H, **L4**-H), 8.28 (d, $J$ = 8.0 Hz, 2H, **L4**-H), 8.04 (d, $J$ = 8.0 Hz, 2H, **L4**-H), 7.96 (d, $J$ = 8.0 Hz, 2H, **L4**-H), 7.62 (d, $J$ = 8.0 Hz, 2H, **L4**-H), 7.53–7.44 (m, 5H, **L4**-H), 7.38 (d, $J$ = 8.0 Hz, 2H, **L4**-H), 7.22 (d, $J$ = 8.0 Hz, 2H, **L4**-H), 7.13 (d, $J$ = 8.0 Hz, 2H, **L4**-H), 6.93–6.85 (m, 7H, **L4**-H), 6.75 (d, $J$ = 8.0 Hz, 2H, **L4**-H), 6.62 (d, $J$ = 8.0 Hz, 2H, **L4**-H), 6.54 (t, $J$ = 8.0 Hz, 2H, **L4**-H), 5.99–5.91 (m, 5H, **L4**-H), 5.39 (d, $J$ = 8.0 Hz, 2H, **L4**-H), 5.16 (s, 2H, **L4**-H), 2.04 (s, 30H, Cp*-H) 1.54 (s, 30H, Cp*-H); $^1$H NMR (400 MHz, DMSO, ppm): 9.43 (d, $J$ = 8.0 Hz, 2H, **L4**-H), 9.33 (s, 2H, pyrazine-H), 8.83 (s, 2H, pyrazine-H), 8.66 (s, 3H, **L4**-H), 8.53–8.49 (m, 9H, **L4**-H), 8.43 (d, $J$ = 12.0 Hz, 2H, **L4**-H), 8.25–8.12 (m, 6H, **L4**-H), 7.92–7.83 (m, 4H, **L4**-H), 1.67 (s, 30H, Cp*-H); elemental analysis (%) calcd for $C_{156}H_{120}F_{12}Rh_4N_{12}O_{12}S_4$ ($M$ = 3122.56): C 60.00, H 3.87, N 5.38; found: C 60.02, H 3.81, N 5.43.


© 2020 Wiley-VCH Verlag GmbH & Co. KGaA, Weinheim

### X-ray crystal structure determinations

The X-ray intensity data for the complexes were collected with a Bruker D8 Venture system at 203 K with the ω-scan technique. The structures were solved and refined with SHELXTL.[20,21]

CCDC 1957680 (**1a**), 1957681 (**1b**), 1957682 (**2**), 1957683 (**3**), and 1957684 (**4**) contain the supplementary crystallographic data for this paper. These data are provided free of charge by The Cambridge Crystallographic Data Centre.

## *Acknowledgements*

This work was supported by the National Science Foundation of China (21531002, 21720102004) and the Shanghai Science and Technology Committee (13JC1400600).

## Conflict of interest

The authors declare no conflict of interest.

**Keywords:** C–H activation · molecular tweezers · polyaromatic ligands · rhodium · supramolecular chemistry

[1] a) X. Ji, M. Ahmed, L. Long, N. M. Khashab, F. Huang, J. L. Sessler, *Chem. Soc. Rev.* **2019**, *48*, 2682 – 2697; b) P. Molina, F. Zapata, A. Caballero, *Chem. Rev.* **2017**, *117*, 9907 – 9972; c) W. B. Motherwell, R. B. Moreno, I. Pavlakos, J. R. T. Arendorf, T. Arif, G. J. Tizzard, S. J. Coles, A. E. Aliev, *Angew. Chem. Int. Ed.* **2018**, *57*, 1193 – 1198; *Angew. Chem.* **2017**, *130*, 1207 – 1212; d) A. Harada, Y. Takashima, M. Nakahata, *Acc. Chem. Res.* **2014**, *47*, 2128 – 2140.

[2] a) D. Guin, M. Gruebele, *Chem. Rev.* **2019**, *119*, 10691 – 10717; b) H.-X. Zhou, X. Pang, *Chem. Rev.* **2018**, *118*, 1691 – 1741; c) V. R. Mundlapati, D. K. Sahoo, S. Bhaumik, S. Jena, A. Chandrakar, H. S. Biswal, *Angew. Chem. Int. Ed.* **2018**, *57*, 16496 – 16500; *Angew. Chem.* **2018**, *130*, 16734 – 16738; d) D. Wang, B. Liu, Y. Ma, C. Wu, Q. Mou, H. Deng, R. Wang, D. Yan, C. Zhang, X. Zhu, *J. Am. Chem. Soc.* **2017**, *139*, 14021 – 14024.

[3] a) M. A. B. Ferreira, J. D. J. Silva, S. Grosslight, A. Fedorov, M. S. Sigman, C. Copéret, *J. Am. Chem. Soc.* **2019**, *141*, 10788 – 10800; b) H. Wang, Y. Park, Z. Bai, S. Chang, G. He, G. Chen, *J. Am. Chem. Soc.* **2019**, *141*, 7194 – 7201; c) S. Yamada, *Chem. Rev.* **2018**, *118*, 11353 – 11143; d) K. Lee, D. L. Silverio, S. Torker, D. W. Robbins, F. Haeffner, F. W. van der Mei, A. H. Hoveyda, *Nat. Chem.* **2016**, *8*, 768 – 777.

[4] a) D. Niu, Y. Jiang, L. Ji, G. Ouyang, M. Liu, *Angew. Chem. Int. Ed.* **2019**, *58*, 5946 – 5950; *Angew. Chem.* **2019**, *131*, 6007 – 6011; b) E. S. Epstein, L. Martinetti, R. H. Kollarigowda, O. C.-D. L. Torre, J. S. Moore, R. H. Ewoldt, P. V. Braun, *J. Am. Chem. Soc.* **2019**, *141*, 3597 – 3604; c) S. E. Wheeler, T. J. Seguin, Y. Guan, A. C. Doney, *Acc. Chem. Res.* **2016**, *49*, 1061 – 1069; d) X. Wang, J. Hu, G. Liu, J. Tian, H. Wang, M. Gong, S. Liu, *J. Am. Chem. Soc.* **2015**, *137*, 15262 – 15275.

[5] a) S. Datta, M. L. Saha, P. J. Stang, *Acc. Chem. Res.* **2018**, *51*, 2047 – 2063; b) S. Pullen, G. H. Clever, *Acc. Chem. Res.* **2018**, *51*, 3052 – 3064; c) C. R. Kim, T. Uemura, S. Kitagawa, *Chem. Soc. Rev.* **2016**, *45*, 3828 – 3845; d) A. J. McConnell, C. S. Wood, P. P. Neelakandan, J. R. Nitschke, *Chem. Rev.* **2015**, *115*, 7729 – 7793; e) S. De, K. Mahata, M. Schmittel, *Chem. Soc. Rev.* **2010**, *39*, 1555 – 1575; f) C. G. Oliveri, P. A. Ulmann, M. J. Wiester, C. A. Mirkin, *Acc. Chem. Res.* **2008**, *41*, 1618 – 1629; g) T. R. Cook, P. J. Stang, *Chem. Rev.* **2015**, *115*, 7001 – 7045.

[6] a) W. Cullen, H. Takezawa, M. Fujita, *Angew. Chem. Int. Ed.* **2019**, *58*, 9171 – 9173; *Angew. Chem.* **2019**, *131*, 9269 – 9271; b) S. K. Mohan Nalluri, J. Zhou, T. Cheng, Z. Liu, M. T. Nguyen, T. Chen, H. A. Patel, M. D. Krzyaniak, W. A. Goddard III, M. R. Wasielewski, J. F. Stoddart, *J. Am. Chem. Soc.* **2019**, *141*, 1290 – 1303; c) F. J. Rizzuto, J. P. Carpenter, J. R. Nitschke, *J. Am. Chem. Soc.* **2019**, *141*, 9087 – 9095; d) B. S. Pilgrim, D. A. Roberts, T. G. Lohr, T. K. Ronson, J. R. Nitschke, *Nat. Chem.* **2017**, *9*, 1276 – 1281.

[7] a) T. Sawada, A. Saito, K. Tamiya, K. Shimokawa, Y. Hisada, M. Fujita, *Nat. Commun.* **2019**, *10*, 921 – 927; b) T. Prakasam, A. Devaraj, R. Saha, M. Lusi, J. Brandel, D. Esteban-Gómez, C. Platas-Iglesias, M. A. Olson, P. S. Mukherjee, A. Trabolsi, *ACS Catal.* **2019**, *9*, 1907 – 1914; c) J. J. Danon, D. A. Leigh, S. Pisano, A. Valero, I. J. Vitorica-Yrezabal, *Angew. Chem. Int. Ed.* **2018**, *57*, 13833 – 13837; *Angew. Chem.* **2018**, *130*, 14029 – 14033; d) F. B. L. Cougnon, K. Caprice, M. Pupier, A. Bauzá, A. Frontera, *J. Am. Chem. Soc.* **2018**, *140*, 12442 – 12450.

[8] a) M. Park, K.-I. Hong, M. Kang, T.-W. Kim, H. Lee, W.-D. Jang, K.-U. Jeong, *ACS Nano* **2019**, *13*, 6101 – 6112; b) Y. Hisamatsu, N. Umezawa, H. Yagi, K. Kato, T. Higuchi, *Chem. Sci.* **2018**, *9*, 7455 – 7467; c) F.-G. Klärner, T. Schrader, *Acc. Chem. Res.* **2013**, *46*, 967 – 978; d) M. Hardouin-Lerouge, P. Hudhomme, M. Salle, *Chem. Soc. Rev.* **2011**, *40*, 30 – 43; e) M. Harmata, *Acc. Chem. Res.* **2004**, *37*, 862 – 873; f) C.-W. Chen, H. W. Whitlock, Jr., *J. Am. Chem. Soc.* **1978**, *100*, 4921 – 4922.

[9] a) E. Kirchner, D. Bialas, F. Fennel, M. Grüne, F. Würthner, *J. Am. Chem. Soc.* **2019**, *141*, 7428 – 7438; b) L. Li, N. Erwin, S. Möbitz, F. Niemeyer, T. Schrader, R. H. A. Winter, *Chem. Eur. J.* **2019**, *25*, 9827 – 9833; c) K. Takaishi, T. Okuyama, S. Kadosaki, M. Uchiyama, T. Ema, *Org. Lett.* **2019**, *21*, 1397 – 1401; d) C. Heid, A. Sowislok, T. Schaller, F. Niemeyer, F.-G. Klärner, T. Schrader, *Chem. Eur. J.* **2018**, *24*, 1 – 13; e) X. Zhang, L. Ao, Y. Han, Z. Gao, F. Wang, *Chem. Commun.* **2018**, *54*, 1754 – 1757; f) H. M. Colquhoun, Z. Zhu, *Angew. Chem. Int. Ed.* **2004**, *43*, 5040 – 5045; *Angew. Chem.* **2004**, *116*, 5150 – 5155.

[10] a) Z. Gao, Y. Han, Z. Gao, F. Wang, *Acc. Chem. Res.* **2018**, *51*, 2719 – 2729; b) S. Ibáñez, M. Poyatos, E. Peris, *Angew. Chem. Int. Ed.* **2017**, *56*, 9786 – 9790; *Angew. Chem.* **2017**, *129*, 9918 – 9922; c) C. Biz, S. Ibáñez, M. Poyatos, D. Gusev, E. Peris, *Chem. Eur. J.* **2017**, *23*, 14439 – 14444; d) Y.-K. Tian, Y.-G. Shi, Z.-S. Yang, F. Wang, *Angew. Chem. Int. Ed.* **2014**, *53*, 6090 – 6094; *Angew. Chem.* **2014**, *126*, 6204 – 6208.

[11] a) V. Valderreya, G. Aragaya, P. Ballester, *Coord. Chem. Rev.* **2014**, *258 – 259*, 137 – 156; b) H. Yoon, J. M. Lim, H.-C. Gee, C.-H. Lee, Y.-H. Jeong, D. Kim, W.-D. Jang, *J. Am. Chem. Soc.* **2014**, *136*, 1672 – 1679; c) S. Olsson, C. Schäfer, M. Blom, A. Gogoll, *ChemPlusChem* **2018**, *83*, 1169 – 1178; d) X. Li, M. Tanasova, C. Vasileiou, B. Borhan, *J. Am. Chem. Soc.* **2008**, *130*, 1885 – 1893.

[12] a) W.-X. Gao, H.-N. Zhang, G.-X. Jin, *Coord. Chem. Rev.* **2019**, *386*, 69 – 84; b) Y. Lu, H.-N. Zhang, G.-X. Jin, *Acc. Chem. Res.* **2018**, *51*, 2148 – 2158; c) Y.-Y. Zhang, W.-X. Gao, L. Lin, G.-X. Jin, *Coord. Chem. Rev.* **2017**, *344*, 323 – 344; d) Y.-F. Han, G.-X. Jin, *Acc. Chem. Res.* **2014**, *47*, 3571 – 3579.

[13] a) W.-L. Shan, Y.-J. Lin, F. E. Hahn, G.-X. Jin, *Angew. Chem. Int. Ed.* **2019**, *58*, 5882 – 5886; *Angew. Chem.* **2019**, *131*, 5941 – 5946; b) L.-L. Dang, Z.-B. Sun, W.-L. Shan, Y.-J. Lin, Z.-H. Li, G.-X. Jin, *Nat. Commun.* **2019**, *10*, 2057 – 2065; c) W.-X. Gao, H.-J. Feng, Y.-J. Lin, G.-X. Jin, *J. Am. Chem. Soc.* **2019**, *141*, 9160 – 9164; d) Y. Lu, Y.-X. Deng, Y.-J. Lin, Y.-F. Han, L.-H. Weng, Z.-H. Li, G.-X. Jin, *Chem* **2017**, *3*, 110 – 121.

[14] a) B.-B. Guo, W.-X. Gao, Y.-J. Lin, G.-X. Jin, *Dalton Trans.* **2018**, *47*, 7701 – 7708; b) L. Zhang, H. Li, L.-H. Weng, G.-X. Jin, *Organometallics* **2014**, *33*, 587 – 593; c) W.-B. Yu, Y.-F. Han, Y.-J. Lin, G.-X. Jin, *Chem. Eur. J.* **2011**, *17*, 1863 – 1871; d) Y.-F. Han, H. Li, L.-H. Weng, G.-X. Jin, *Chem. Commun.* **2010**, *46*, 3556 – 3558.

[15] L. Zhang, L. Lin, D. Liu, Y.-J. Lin, Z.-H. Li, G.-X. Jin, *J. Am. Chem. Soc.* **2017**, *139*, 1653 – 1660.

[16] C. White, A. Yates, P. M. Maitlis, *Inorg. Synth.* **1992**, *29*, 228 – 234.

[17] S. Samanta, A. D. Gupta, A. K. Mallik, *Monatsh. Chem.* **2014**, *145*, 1669 – 1673.

[18] P. K. Sahoo, C. Giri, T. S. Haldar, R. Puttreddy, K. Rissanen, P. Mal, *Eur. J. Org. Chem.* **2016**, 1283 – 1291.

[19] X.-B. Shao, X.-K. Jiang, X. Zhao, C.-X. Zhao, Y. Chen, Z.-T. Li, *J. Org. Chem.* **2004**, *69*, 899 – 907.

[20] SHELXS-97: G. M. Sheldrick, *Acta Crystallogr. Sect. A* **1990**, *46*, 467 – 473.

[21] SHELXS-97: G. M. Sheldrick, *Acta Crystallogr. Sect. A* **2008**, *64*, 112 – 122.

Manuscript received: October 7, 2019
Revised manuscript received: November 3, 2019
Accepted manuscript online: November 6, 2019
Version of record online: December 12, 2019


© 2020 Wiley-VCH Verlag GmbH & Co. KGaA, Weinheim